Direct Observation of Sub-100 fs Mobile Charge Generation in a Polymer-Fullerene Film

D. G. Cooke

Department of Physics, McGill University, Montreal, Canada H3A 2T8

F. C. Krebs

Department of Energy Conversion and Storage, Technical University of Denmark, DK-4000, Roskilde, Denmark

P. U. Jepsen

Department of Photonics Engineering, Technical University of Denmark, DK-2800, Kongens Lyngby, Denmark
(Received 30 August 2011; published 31 January 2012; corrected 7 February 2012)

The formation of mobile charges in a roll-to-roll processed poly-3-hexylthiophene–fullerene bulk heterojunction film is observed directly by using transient terahertz spectroscopy with sub-100 fs temporal resolution. The transient terahertz ac conductivity reveals that 20% of the incident pump photons are converted into highly delocalized charges within the 40 fs, 3.1 eV pump pulse duration, which then rapidly becomes localized within 120 fs. Approximately 2/3 of these carriers subsequently decay, possibly into an exciton, on a 1 ps time scale.

Semiconducting conjugated polymers are promising materials for mass-produced and inexpensive solar cells and organic light-emitting diodes [1,2]. The potential for cheaper, lighter, and flexible polymer-based devices has driven a massive research effort investigating their basic photophysical properties [3]. The mechanisms for charge generation, recombination, and transport in these materials, however, are still far from understood, particularly in the femtoseconds to picoseconds following photon absorption [4]. In device films, charge generation is facilitated by the bulk heterojunction (BHJ) scheme where the polymer (usually the donor) is blended with an acceptor material. The strong local field at the distributed donor-acceptor interface facilitates charge transfer and exciton dissociation. Femtosecond transient absorption (TA) measurements of polymer:fullerene films have shown charge transfer to fullerenes as early as 45 fs after photon absorption [5]. However, these charges are not yet necessarily free. Binding energies on the order of 0.1–0.5 eV are expected between electrons transferred to the acceptor and holes remaining on the donor, which must be overcome before the charges can be fully dissociated [4].

The microscopic mobility of carriers was recently identified as an important determining factor in geminate recombination versus free dissociation in a BHJ film [6]. Despite its importance, however, there have been no measurements that both are intrinsically sensitive to mobile carriers and simultaneously have sufficient sub-100 fs resolution to directly resolve their creation. TA measurements that have sufficient temporal resolution show spectrally broad, overlapping signatures that have been assigned to delocalized polarons [7], but this interpretation remains strongly debated [4]. Several groups argue that the perturbation to the polaron absorption spectra due to the small

Coulomb binding energy is negligible, and thus free and bound polarons are indistinguishable by TA [8–10]. The photocurrent cross-correlation method is capable of discerning free from bound polaron dynamics in the small signal limit; however, the temporal resolution to date has been limited to >300 fs [10]. In this Letter, we demonstrate a technique intrinsically sensitive to mobile carriers with sub-100 fs resolution and directly resolve the creation of mobile charges in a BHJ film.

Time-resolved terahertz spectroscopy (TRTS) has demonstrated itself as a powerful tool for investigating the picosecond conductivity dynamics of conjugated polymers and organic conductors [11–17]. To date, however, measurements on conjugated polymers have been unable to compete with TA in terms of temporal resolution, being limited to times >300 fs by the dispersion present in the nonlinear terahertz (THz) generation and detection crystals. In this Letter, we demonstrate that TRTS can directly identify intrinsic sub-100 fs creation dynamics of mobile charge carriers in a BHJ polymer film by using a dispersionless air-plasma generation and detection scheme. We investigate the <2 ps mobile carrier dynamics in the technologically important polymer poly-3-hexylthiophene (P3HT) blended with the acceptor phenyl-C60-butyric acid methyl ester (PCBM). To the best of our knowledge, this is the first ultrafast optical study of an actual device-ready, roll-to-roll processed BHJ film fabricated by a method amenable to mass production. We find that, for these films, 20% of the incident photons are converted to delocalized charge carriers which rapidly partially localize. Subsequently, 2/3 of these carriers relax to a completely localized state or charge neutral state (exciton) within 1 ps, while the rest remain mobile on a much longer time scale.

Device and sample films were prepared simultaneously by using differentially pumped slot-die coating, described in more detail elsewhere [18]. A solution of P3HT (Sepiolid P200, 30 mg mL^{-1}) and PCBM (Solenne 99%, 30 mg mL^{-1}) was prepared in chlorobenzene and slot-die coated into stripes with a width of 13 mm on a 130 μm thick polyethyleneterphthalate (PET) substrate. The substrate was prepatterned with indium tin oxide (ITO) prepared as described earlier [1,19]. The ITO had a 25 nm thick layer of ZnO on top prepared by slot-die coating as an electron transport layer, and a thick active layer was coated directly on top. Along a stripe, one has access to PET-ITO-ZnO and PET-ZnO. After coating the active layer, a thin hole transport layer of poly(ethylene-3,4-dioxy-thiophene):polystyrenesulphonate (PEDOT:PSS) was coated on top followed by screen printing of a silver grid electrode. The films were annealed at 140 °C for 10 min due to the roll-to-roll process, which requires several heating steps post film formation. The devices were then tested and typically gave a power conversion efficiency of 1.7% for 800 nm thick active layers under 1.5 AMG illumination. The device films were cut after testing the performance in the region of the functional solar cell (PET-ITO-ZnO-P3HT:PCBM-PEDOT:PSS-Ag) and immediately next to it (PET-ZnO- P3HT:PCBM-PEDOT:PSS). The latter films were used in this work as the THz probe pulse does not penetrate through the ITO or Ag coatings.

We apply ultrabroadband TRTS in normal incidence reflection mode and record the full THz pulse waveforms at different pump-probe delay times τ_p. The temporal resolution of TRTS in this mode is not dictated by the duration of the THz pulses but rather by a combination of the pump pulse duration and dispersion in both the generation and detection media [20]. Here we have eliminated the effects of dispersion, leaving the temporal resolution governed solely by the pump pulse duration. A transient THz spectrometer was constructed based on laser-induced plasma generation. The 1.5 mJ, 40 fs pulses from a Ti: sapphire regenerative laser amplifier are split into three beams in a 40/40/20 ratio. One of the more intense beams is used to create a second harmonic pulse in a 100 μm thick beta barium borate crystal. An off-axis parabolic mirror focuses the copropagating 800 and 400 nm pulses to create a laser-induced plasma in dry nitrogen, emitting a broadband THz transient through a combination of four-wave mixing and nonlinear laser-field driven currents in the plasma [21,22]. The ultrabroadband THz pulse is collimated and focused onto the sample which is pumped colinearly by second harmonic 400 nm pulses from a 100 μm thick beta barium borate nonlinear crystal. The pump spot size on the sample was 1.5 mm diameter (full width at half maximum), and the fluence was 570 μJ/cm^2. No film degradation was observed at this pump power; however, bleaching was seen at higher power. The weaker split-off 800 nm beam is used to sample the THz pulse

electric field by using an air-biased coherent detection scheme similar to that described elsewhere [23]. At each τ_p, the reflected THz pulse is recorded in the presence of the pump pulse $E_{pump}(\tau_p, t)$, and the differential, $\Delta E(\tau_p, t) = E_{pump}(\tau_p, t) - E_{ref}(t)$, THz waveforms are acquired simultaneously by using a double modulation scheme that eliminates the effect of laser drift on the measurements [24]. $E_{ref}(t)$ is the THz pulse at negative τ_p. Scanning the THz pulse generation delay line with respect to a fixed pump and sampling beam, we project the THz waveforms such that each point of the measured waveform has experienced an identical τ_p [20,25].

Figure 1(a) shows the Fourier amplitude spectrum of $E_{ref}(t)$ shown in Fig. 1(b). The pulse has components stretching out to 15 THz, more than 6 times that used to previously investigate THz conductivity dynamics in conjugated polymers [13–17,26]. The differential $\Delta E(\tau_p, t)$ is shown in Fig. 1(c) for τ_p from -40 to $+160$ fs. The maximum $\Delta E(t)$ signal of 3.7% of the peak reference pulse is reached after only 120 fs following the arrival of the pump pulse, indicating that the photoexcited mobile charge carrier population is completely developed by this time. More information can be extracted from the transient complex ac conductivity $\tilde{\sigma}(\omega) = \sigma_1(\omega) + i\sigma_2(\omega)$. The
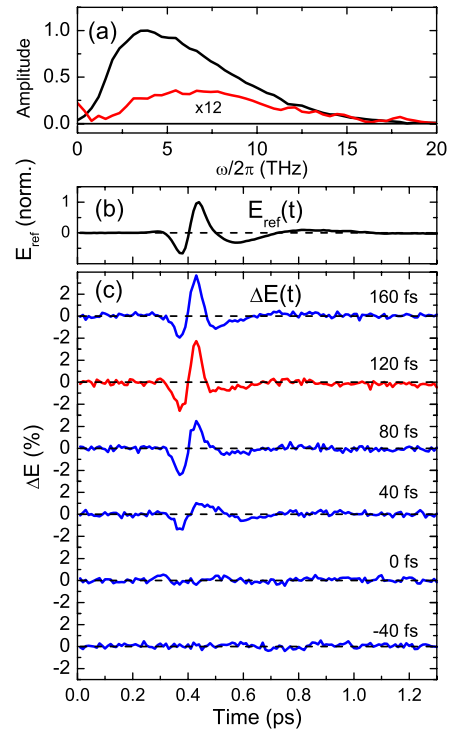

FIG. 1 (color online). (a) Fourier amplitude spectrum of the reference (solid black line) and differential (red line) $\Delta E(\omega, 120 \text{ fs}) \times 12$ THz pulses. (b) Reflected THz transient from the unexcited polymer sample and (c) short time evolution of the differential reflected THz signal for pump-probe delay steps of 40 fs.

Fourier transforms of the $\Delta E(\tau_p, t)$ and $E_{\text{ref}}(t)$ transients are related to the $\tilde{\sigma}(\omega, \tau_p)$ of the thin photoconductive film on the insulating substrate by [27]

$$1 + \frac{\Delta E(\omega, \tau_p)}{E_{\text{ref}}(\omega)} = \left(\frac{1 - n - Z_0 d\tilde{\sigma}(\omega, \tau_p)}{1 + n + Z_0 d\tilde{\sigma}(\omega, \tau_p)}\right)\left(\frac{1 + n}{1 - n}\right), \quad (1)$$

where n is the index of refraction of the PET substrate, taken as $n = 1.7$ [28]. Z_0 is the impedance of free space (377 Ω), and d is the 260 nm thickness of the photoexcited film, approximated by the pump absorption depth of the BHJ film at the 400 nm pump wavelength [16]. The extracted $\tilde{\sigma}(\omega, \tau_p)$ is shown in Fig. 2. The $\sigma_1(\omega, \tau_p)$ spectrum is suppressed at low frequency and increases monotonically over the THz bandwidth with no sign of the saturation predicted in a microscopic hopping model used to describe the THz $\tilde{\sigma}(\omega)$ observed in a previous, lower bandwidth TRTS study [29] of polyphenylene:fullerene films. The negative, capacitive $\sigma_2(\omega, \tau_p)$ spectra

FIG. 2 (color online). The short time evolution of the complex conductivity for indicated τ_p. Red and blue lines are complex-valued fits to the Drude-Smith model described in the text.

show some positive curvature, indicating a return to a positive, Drude-like inductive response at still higher ω. We attribute these spectra as signatures of mobile charges, as in previous studies in the 0.1–2.5 THz range [13,15,16]. The interpretation of the conductivity spectra can take two avenues: (i) as the low energy tail of discrete transitions for delocalized polarons that are inhomogeneously broadened due to disorder [30] or (ii) hopping-type transport of mobile charges in a disordered film where hopping between pairs of states dominates [31]. Our data cannot distinguish between these two pictures, as both energetic and structural disorder can lead to the type of spectra observed here. However, regardless of the specific model for the functional form of $\tilde{\sigma}(\omega)$, the general identification with mobile charges is clear. Thus we observe the unambiguous creation of mobile charge carriers in a bulk heterojunction film on sub-100 fs time scales for the first time.

We find that we can accurately describe $\tilde{\sigma}(\omega, \tau_p)$ for $\tau_p \gtrsim 40$ fs resolution of our experiment by a classical Drude-Smith model that has been extensively applied to the THz conductivity of disordered systems including conjugated polymers [15,16]. In this phenomenological model, the conductivity is given by [32]

$$\tilde{\sigma}(\omega) = \frac{\omega_p^2 \epsilon_0 \tau}{1 - i\omega\tau}\left(1 + \frac{c}{1 - i\omega\tau}\right), \quad (2)$$

where ω_p is the plasma frequency, τ is the carrier momentum relaxation time, and the effect of disorder is parameterized by the constant c [33]. By taking negative c values approaching -1, the current response function $j(t)$ resembles an overdamped harmonic oscillator, which has been pointed out is a signature of any realistic hopping model [34]. The Drude-Smith model can also reproduce functional forms of $\tilde{\sigma}(\omega)$ derived from interband transitions in the limit of $c = -1$, as was discussed in Ref. [32]. Simultaneous Drude-Smith model fits to σ_1 and σ_2 are shown in Fig. 2 for $\tau_p \gtrsim 40$ fs. At $\tau_p = 40$, 80, and 120 fs, we observe a Drude-type response with $c = -0.02$, -0.59, and -0.82, respectively. For $\tau_p > 120$ fs, both τ and the c parameter are constant at 7 fs and -0.91. Thus, immediately after injection, carriers are highly delocalized and rapidly become partially localized within 120 fs, in agreement with a recent work [35]. The plasma frequency ω_p is time-dependent as charge carriers become trapped or recombine and peaks at $\omega_p/2\pi = 18.9$ THz. Taking an effective mass $m^* = 1.7\ m_e$ [16], the peak ω_p corresponds to a carrier density of 7.5×10^{18} cm^{-3}. Comparing to the pump photon flux yields an ultrafast photon to mobile carrier conversion efficiency of $\sim 20\%$ considering pump losses. The THz carrier mobility is given by $\mu_{\text{THz}} = e\tau/m^* = 7.2$ cm^2/V s. At THz frequencies, charge carriers scan over much smaller domains and approach the intrinsic polymer chain mobility [36].

The carrier dynamics can be represented by the integrated $\sigma_1(\omega)$ (between 1 and 8 THz) plotted in Fig. 3,
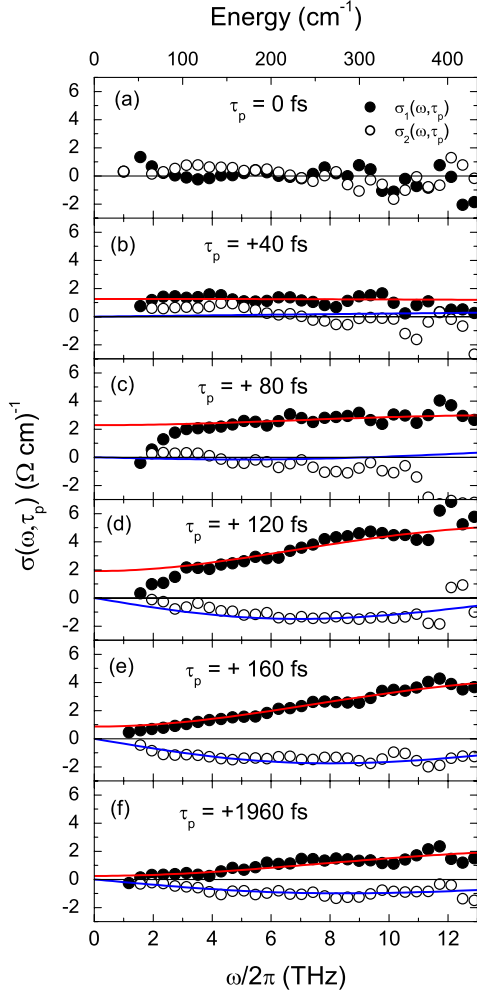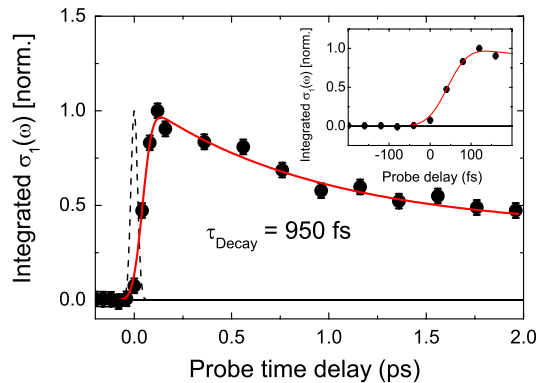
FIG. 3 (color online).   Spectrally integrated $\sigma_1(\omega)$ normalized to the peak value, with the pump pulse envelope depicted at $t = 0$ (40 fs FWHM). The solid red line is an exponential decay convoluted with a 95 fs FWHM response function. The inset is a zoomed view of the rise with convolution fit.

normalized to the peak value. We find that this can be fit by a 95 fs FWHM Gaussian response function convoluted with a 950 fs exponential decay and a long-lived component comprising 34% of the signal not resolved by our scan length. The rise time is shown clearly in the inset in Fig. 3 and is larger than our estimated temporal resolution given the pump pulse duration of 40 fs (dotted line in Fig. 3), so we attribute this to the intrinsic material response. We note that this is in good agreement with TA measurements of the interchain charge pair generation time in both neat and fullerene-blended polythiophenes [37], which also reported a ~20% yield similar to our measurements. This would suggest that, for our excitation conditions, all charge pairs are initially delocalized. There are several scenarios that could explain the rapid, sub-100 fs mobile polaron formation for our excitation conditions. The high photon flux required for these measurements (4.3×10^{19} cm^{-3}) is above the reported threshold for nonlinear processes (2×10^{17} cm^{-3}) [37]; however, we observe a linear dependence with pump power (not shown) rather than the expected superlinear dependence, and so we conclude that this is not a strong effect. Photoexcitation at 400 nm (3.1 eV) compared to the 1.9 eV band gap of the P3HT creates a hot exciton population with ~1.2 eV excess energy which could be used to dissociate the exciton on a 100 fs time scale before thermalization. Indeed, charge separation times as short as 35 fs have been predicted [38,39]. While hot exciton dissociation has previously been used to explain THz conductivity dynamics in 1-methoxy-4-(2-ethylhexyloxy)phenylenevinylene and P3HT films [13,14], predicted photocarrier yields for this mechanism are low (10^{-2}) [8]. As the Drude-Smith model satisfies the Kramers-Kronig relations and therefore the sum rule, the disorder-driven shift of spectral weight from dc to higher frequencies does not affect the extracted ω_p. Thus, we believe that the calculated yield of 20% is accurate and may be too large to be explained by hot

exciton dissociation alone, although we cannot conclusively rule this out without further investigations of the pump energy dependence. The fast ~1 ps decay can be attributed to the formation of an exciton, as was recently suggested in another work investigating P3HT excited with excess photon energy [35].

In conclusion, we have used air-based time-resolved terahertz spectroscopy to directly observed the generation of delocalized charge carriers on sub-100 fs time scales in P3HT–fullerene roll-to-roll processed films. Delocalized charges are created within the pump pulse envelope, after which they rapidly localize on a 120 fs time scale. Approximately 2/3 of these charge carriers subsequently decay to form an exciton on a 1 ps time scale, while the remainder are mobile on much longer time scales.

[1] F. C. Krebs *et al.*, Nanoscale **2**, 873 (2010).
[2] G. Dennler *et al.*, Adv. Mater. **21**, 1323 (2009).
[3] G. Lanzani, *Photophysics of Molecular Materials* (Wiley-VCH, Weinheim, 2006).
[4] T. M. Clarke and J. R. Durrant, Chem. Rev. **110**, 6736 (2010).
[5] C. J. Brabec *et al.*, Chem. Phys. Lett. **340**, 232 (2001).
[6] S. K. Pal *et al.*, J. Am. Chem. Soc. **132**, 12 440 (2010).
[7] I. W. Hwang *et al.*, J. Phys. Chem. C **112**, 4350 (2008).
[8] C. Silva *et al.*, Phys. Rev. B **64**, 125211 (2001).
[9] V. Gulbinas *et al.*, Phys. Rev. B **76**, 235203 (2007).
[10] J. G. Müller *et al.*, Phys. Rev. B **72**, 195208 (2005).
[11] O. Ostroverkhova *et al.*, Phys. Rev. B **71**, 035204 (2005).
[12] F. A. Hegmann *et al.*, Phys. Rev. Lett. **89**, 227403 (2002).
[13] E. Hendry *et al.*, Phys. Rev. Lett. **92**, 196601 (2004).
[14] E. Hendry *et al.*, Chem. Phys. Lett. **432**, 441 (2006).
[15] X. Ai *et al.*, J. Phys. Chem. B **110**, 25 462 (2006).
[16] P. D. Cunningham and L. M. Hayden, J. Phys. Chem. C **112**, 7928 (2008).
[17] H. Němec *et al.*, J. Phys. Chem. C **112**, 6558 (2008).
[18] J. Alstrup *et al.*, ACS Appl. Mater. Interfaces **2**, 2819 (2010).
[19] F. C. Krebs *et al.*, J. Mater. Chem. **19**, 5442 (2009).
[20] J. T. Kindt and C. A. Schmuttenmaer, J. Chem. Phys. **110**, 8589 (1999).
[21] D. J. Cook and R. M. Hochstrasser, Opt. Lett. **25**, 1210 (2000).
[22] M. Kress *et al.*, Opt. Lett. **29**, 1120 (2004).
[23] J. Dai, X. Xie, and X. C. Zhang, Phys. Rev. Lett. **97**, 103903 (2006).
[24] K. Iwaszczuk *et al.*, Opt. Express **17**, 21 969 (2009).
[25] C. Larsen *et al.*, J. Opt. Soc. Am. B **28**, 1308 (2011).
[26] P. Parkinson *et al.*, Phys. Rev. B **78**, 115321 (2008).
[27] J. L. Tomaino *et al.*, Opt. Express **19**, 141 (2011).
[28] P. U. Jepsen *et al.*, Opt. Express **16**, 9318 (2008).

[29] H. Němec *et al.*, Phys. Rev. B **79**, 245326 (2009).

[30] R. Österbacka *et al.*, Science **287**, 839 (2000).

[31] J. C. Dyre, J. Appl. Phys. **64**, 2456 (1988).

[32] N. V. Smith, Phys. Rev. B **64**, 155106 (2001).

[33] This relation can be derived in the impulse response formalism where $\tilde{\sigma}(\omega) = \int_0^\infty j(t)e^{i\omega t}dt$ by assuming a modified current density response from the typical exponential Drude form to be $j(t)/j(0) = f(t/\tau)e^{-t/\tau}$. Here $f(t/\tau)$ can be any unknown differentiable function that modifies the Drude exponential decay. A Taylor expansion about $t = 0$ and subsequent Fourier transformation immediately yield Eq. (2) to first order, where the c parameter is merely the first Taylor coefficient of the unknown function.

[34] J. C. Dyre and T. B. Schrøder, Rev. Mod. Phys. **72**, 873 (2000).

[35] N. Banerji *et al.*, J. Phys. Chem. C **115**, 9726 (2011).

[36] F. Laquai *et al.*, Phil. Trans. R. Soc. A **365**, 1473 (2007).

[37] A. Ruseckas *et al.*, Chem. Phys. Lett. **322**, 136 (2000).

[38] V. I. Arkhipov, E. V. Emelianova, and H. Bassler, Phys. Rev. Lett. **82**, 1321 (1999).

[39] D. M. Basko and E. M. Conwell, Phys. Rev. B **66**, 155210 (2002).